

Jacek Walkowiak | Yan Lu | Michael Gradzielski | Stefan Zauscher |
Matthias Ballauff

Thermodynamic Analysis of the Uptake of a Protein in a Spherical Polyelectrolyte Brush

Suggested citation referring to the original publication:
Macromolecular Rapid Communications 41 (2020) 1
DOI <https://doi.org/10.1002/marc.201900421>
ISSN (print): 1022-1336
ISSN (online): 1521-3927

Postprint archived at the Institutional Repository of the Potsdam University in:
Postprints der Universität Potsdam
Mathematisch-Naturwissenschaftliche Reihe ; 1176
ISSN 1866-8372
<https://nbn-resolving.org/urn:nbn:de:kobv:517-opus4-517307>
DOI <https://doi.org/10.25932/publishup-51730>



Thermodynamic Analysis of the Uptake of a Protein in a Spherical Polyelectrolyte Brush

Jacek Walkowiak, Yan Lu, Michael Gradzielski, Stefan Zauscher, and Matthias Ballauff*

A thermodynamic study of the adsorption of Human Serum Albumin (HSA) onto spherical polyelectrolyte brushes (SPBs) by isothermal titration calorimetry (ITC) is presented. The SPBs are composed of a solid polystyrene core bearing long chains of poly(acrylic acid). ITC measurements done at different temperatures and ionic strengths lead to a full set of thermodynamic binding constants together with the enthalpies and entropies of binding. The adsorption of HSA onto SPBs is described with a two-step model. The free energy of binding ΔG_b depends only weakly on temperature because of a marked compensation of enthalpy by entropy. Studies of the adsorbed HSA by Fourier transform infrared spectroscopy (FT-IR) demonstrate no significant disturbance in the secondary structure of the protein. The quantitative analysis demonstrates that counterion release is the major driving force for adsorption in a process where proteins become multivalent counterions of the polyelectrolyte chains upon adsorption. A comparison with the analysis of other sets of data related to the binding of HSA to polyelectrolytes demonstrates that the cancellation of enthalpy and entropy is a general phenomenon that always accompanies the binding of proteins to polyelectrolytes dominated by counterion release.

The interaction of proteins with synthetic polyelectrolytes in aqueous solution has been a long-standing subject in colloid and polymer science with a large number of papers dealing with the subject.^[1–5] Polyelectrolytes are known to form complex coacervates with proteins of opposite charge and the formation of these complexes strongly depends on the ionic strength of the system.^[4,6] Often complex formation is followed by precipitation and phase separation,^[1,4,6,7] and possible non-equilibrium

states typically render the thermodynamic analysis difficult. Nevertheless, the interaction of highly charged biopolymers such as DNA or RNA with specific proteins has been under intense scrutiny because of its obvious biological relevance.^[8–18]

Work along these lines revealed that binding is often brought about by counterion release^[5,8,19–22] when a patch of positively charged groups on the surface of the protein interacts with the highly charged biopolymer. Thus, this patch now balances the charge of the polyelectrolyte so that the counterions condensed to it may be released. The entropy gain by release of the condensed counterions presents a strong driving force for binding that is even operative under physiological conditions. Counterion release has also been identified as major driving force for the binding of synthetic polyelectrolytes to proteins.^[5,23,24]

Our recent work showed that thermodynamics and driving forces of the β -lactoglobulin adsorption on spherical polyelectrolyte brushes (SPBs) with long chains of poly(styrene sulfonate) can be studied expeditiously by isothermal titration calorimetry (ITC).^[5,25] The resulting complexes of the SPB and the protein stay stable in solution and can be studied by a variety of methods, including small angle X-ray Scattering (SAXS).^[26,27] Recently, a first theoretical study on the interaction of proteins with SPBs has been published.^[28] Up to now, however, a comprehensive thermodynamic study of the uptake of proteins into SPBs has been lacking. In particular,

J. Walkowiak
Institut für Chemie und Biochemie
Freie Universität Berlin
Takustraße 3, 14195 Berlin, Germany

Prof. Y. Lu, Prof. M. Ballauff
Soft Matter and Functional Materials
Helmholtz-Zentrum Berlin für Materialien und Energie
Hahn-Meitner-Platz 1, 14109 Berlin, Germany
E-mail: Matthias.ballauff@helmholtz-berlin.de

The ORCID identification number(s) for the author(s) of this article can be found under <https://doi.org/10.1002/marc.201900421>.

© 2019 The Authors. Published by WILEY-VCH Verlag GmbH & Co. KGaA, Weinheim. This is an open access article under the terms of the Creative Commons Attribution License, which permits use, distribution and reproduction in any medium, provided the original work is properly cited.

Prof. Y. Lu
Institute of Chemistry
University of Potsdam
14467 Potsdam, Germany

Prof. M. Gradzielski
Stranski Laboratorium für Physikalische Chemie und Theoretische Chemie
Institut für Chemie
Straße des 17. Juni 124
Sekt. TC7
Technische Universität Berlin
D-10623 Berlin, Germany

Prof. S. Zauscher
Mechanical Engineering and Material Science
Duke University
Durham, NC 27708, USA

DOI: 10.1002/marc.201900421

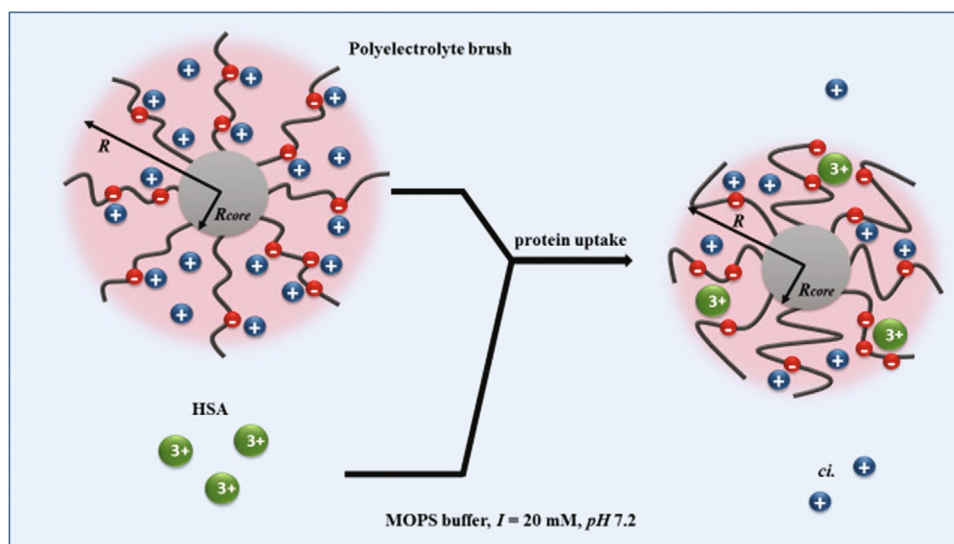


Figure 1. Schematic illustration of a spherical polyelectrolyte brush in the process of protein adsorption. The polyelectrolyte brush consists of a solid polystyrene core (gray sphere) with radius $R_{h,core} = 57$ nm and surface grafted poly(acrylic acid) chains. Red spheres on the PAA chains represent the negative charge of the acidic residues, while blue spheres represent the positive counterions; note the presence of condensed and free counterions within the brush layer. The HSA molecules are represented by green spheres. The radius of the brush $R = 288$ nm decreased after protein adsorption to 196 nm.

no information is available on the dependence of the binding constant on temperature.

Here we present a full thermodynamic analysis of the interaction of proteins with SPBs, bearing chains of poly(acrylic acid) (PAA). As a model protein for this study we chose human serum albumin (HSA) because we already investigated the complex formation of HSA with single chains of poly(acrylic acid) (PAA).^[29] In that study we used ITC to examine the complex formation in aqueous solution by varying both temperature and ionic strength.^[29] The experimental studies were combined with molecular dynamics simulations with explicit counterions. Both, experiments and simulations led to the conclusion that counterion release dominates the formation of the 1:1 complex of PAA and HSA. Moreover, the experimental binding constant coincides with the calculated one within the limits of error. We found that while the free energy of binding, ΔG_b , depended hardly on temperature, the measured enthalpy, ΔH^{ITC} , varied strongly with temperature. Thus, we concluded that binding of HSA to PAA-chains is accompanied by a marked cancellation of enthalpy and entropy that is a common feature for proteins interacting with natural polyelectrolytes.^[10,30–32] The study of the interaction of short, single polyelectrolytes with HSA is thus an excellent starting point for the analysis of the interaction of this protein with more complicated polyelectrolytes, in particular of brush architecture.

Here, we extend this analysis to the interaction of HSA with SPBs in order to obtain the full thermodynamic information on the binding process. The SPBs, shown schematically in **Figure 1**, consist of a solid core particle of approximately 115 nm diameter to which long polyelectrolyte chains are densely grafted.^[3,33,34] When immersed in water, most of the counterions will be confined to the brush layer if the ionic strength is low, that is, in the osmotic limit.^[33] In this limit, proteins are strongly adsorbed within the brush layer whereas at

high salt concentrations only little adsorption takes place.^[24,35] ITC was used to determine the binding constants at different ionic strengths and for a range of temperatures. To ensure that the heat signal is not due to a partial unfolding upon binding, we also studied the complex by FT-IR, where changes in protein secondary structure upon adsorption to the brush layer would show up in the spectra immediately.^[36,37] The analysis of all data obtained here will allow us to present a comprehensive discussion of the driving forces for adsorption, including the role of water in the process.

A series of ITC experiments was performed at eight different temperatures ranging from 25 to 37 °C. The experiments were performed in a buffer solution at constant ionic strength ($I = 20$ mM) and fixed pH of 7.2. Under these conditions both the protein as well as the SPB carry a net negative effective charge. After the evaluation of ITC data as described in the Isothermal Titration Calorimetry section in Experimental Section, the integrated isotherms were fitted with the two set of independent sites (TSIS) model and the results compared to fit results from the single set of identical sites (SSIS) model. We used a semi-logarithmic plot to determine the best fit (see **Figure S5**, Supporting Information).^[38] **Figure 2** shows that the present data are better described by the TSIS model, which assumes the presence of two different binding sites of the SPB for HSA.

This finding, observed previously in the case of SPB interacting with proteins,^[25] may be explained as follows. From the spherical geometry of the SPB particles two regions in the polyelectrolyte brush can be distinguished. The inner region with the higher chain density in which proteins can interact with more than one chain, and the outer region with the lower chain density in which proteins can interact with only one polyelectrolyte chain. In the present case we identify the first binding site by the adsorption of HSA to unoccupied PAA chains of the brush. The second binding site may represent the second

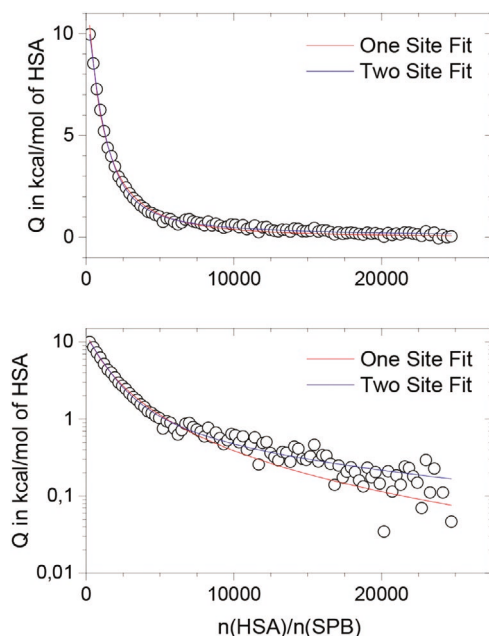


Figure 2. Binding isotherm after double subtraction (corrected for HSA, and SPB heat of dilution) for the adsorption of HSA onto SPB at pH 7.2 ($I = 20$ mM, $T = 27$ °C). The fit quality of different models is demonstrated in a typical ITC plot (top panel) and a semi-logarithmic plot (lower panel).

adsorption step when HSA binds to a PAA chain already occupied by a previously adsorbed protein. Evidently, the first binding step can be investigated with higher accuracy than the second one and the following discussion will be focused on those data. All data obtained with the TSIS model are given in Table S1, Supporting Information.

We used FT-IR spectroscopy to analyze the secondary structure of HSA immobilized onto SPB. FT-IR-spectra are sensitive to changes in the secondary structure that may be caused by the interaction with the polyelectrolyte brush.^[26,36,39–41] The result is shown in Figure S1, Supporting Information. This analysis showed no significant disturbance in the secondary structure of the protein adsorbed on the SPB. We thus conclude that the ITC-signal arises exclusively from the adsorption process and is not due to partial unfolding.

To elucidate the effect of ionic strength on binding, we performed an ITC measurement at 37 °C and $I = 50$ mM. As shown in Figure 3, the measured heat effect decreased dramatically with increasing salt concentration. Therefore, the binding constant at $I = 50$ mM could not be determined with sufficient accuracy.

A similar, strong decrease of binding was reported for short linear PAA binding to HSA.^[29] For higher ionic strengths, the repulsive forces between the SPB and the protein prevail and no adsorption takes place. This can be explained by the following theoretical considerations.^[28] The total free energy of binding can be described as the sum of the *van der Waals* and excluded-volume interaction, the electrostatic contribution, and the counterion release contribution. Only the latter contribution is strongly attractive,^[28] while the electrostatic contribution takes into account the monopolar repulsion and dipolar and Born attraction. The most prominent repulsive contribution is

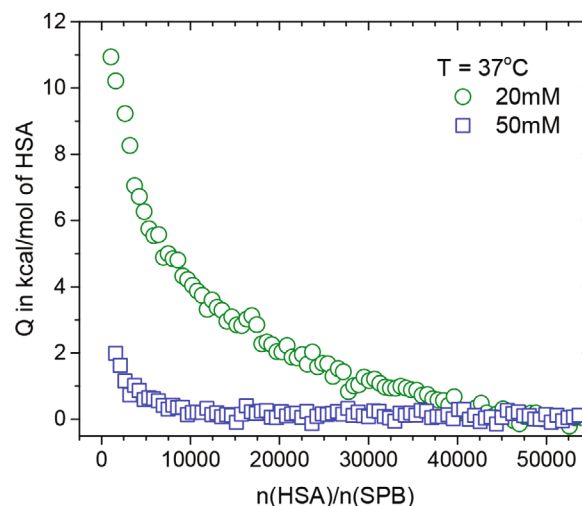


Figure 3. Effect of ionic strength on binding. The integrated heats Q of adsorption of HSA onto SPB at constant temperature of 37 °C for $I = 20$ and 50 mM are displayed.

represented by the excluded volume interaction which is completely dominated by the osmotic contribution of the counterions.^[28] Since we find approximately the same ΔG_b as derived previously^[29] for the interaction of free PAA with HSA, we conclude that the terms related to the brush layer cancel each other out to good approximation. This comparison suggests that the first step of HSA binding onto SPB reflects most likely the interaction of PAA chains with the Sudlow II site of a given protein, as previously found in the analysis of HSA binding to single PAA-chains.^[29]

The effect of pH on binding has been studied by Wittemann et al.^[42] in detail. The pH was found to be an important but not decisive parameter for the protein adsorption to SPBs. The decisive parameter is the ionic strength whereas the pH only modifies the strength of adsorption. For single polyelectrolyte chains, this problem has been studied by Dubin et al.^[4,43] who came to comparable results. Therefore all experiments reported here were done at the optimal pH of 7.2.

Previous studies clearly showed that the temperature dependence of polyelectrolyte binding to protein yields the full thermodynamic information on the binding process.^[5,22,44,45] Figure 4 displays three ITC-isotherms, the remaining data for other temperatures are shown in Figure S4, Supporting Information.

Figure 4 shows that the overall calorimetric enthalpy becomes stronger with increasing temperature. The heat ΔH_i^{ITC} measured directly by ITC increases approximately linearly with increasing temperature (Figure S7, Supporting Information) and reveals a significant positive heat capacity change $\Delta C_{p,\text{ITC}} = 13.7 \pm 1.6$ kJ mol⁻¹ K⁻¹ for the first step of binding and $\Delta C_{p,2,\text{ITC}} = 6.9 \pm 1.7$ kJ mol⁻¹ K⁻¹ for the second step of binding. The results of the fits are listed in Table S1, Supporting Information.

Figure 5a displays the measured binding free energy ΔG_b for the first and the second (Figure S8, Supporting Information) adsorption step, and clearly shows the nonlinear temperature dependence of ΔG_b . The solid lines represent the best fits to Equation (12). The thermodynamic parameters involved in HSA binding onto SPB were derived by analysis with the

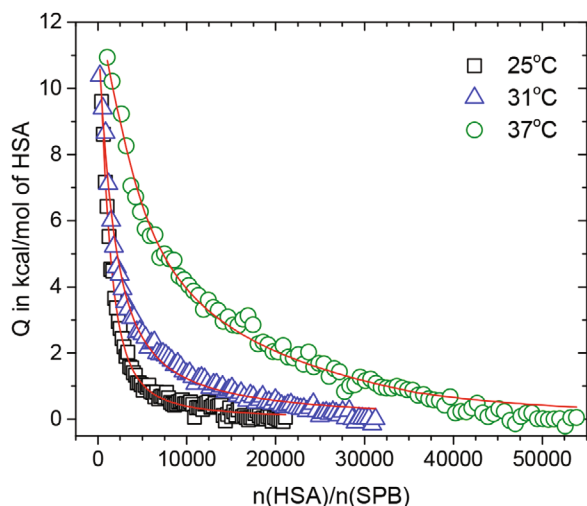


Figure 4. Effect of temperature on binding. The integrated heats, Q , of adsorption of HSA onto SPB at temperatures between 25 and 37 °C at $l = 20$ mm and the respective fits are shown. To improve clarity, data for only three temperatures are displayed.

nonlinear van't Hoff equation (Equation (12)) and the resulting values of ΔS_b , ΔH_b and $\Delta C_{p,vH}$ are listed in Table S1, Supporting Information. These data indicate a large positive heat capacity change $\Delta C_{p1vH} = 12.1 \pm 2.7 \text{ kJ mol}^{-1} \text{ K}^{-1}$ for the first step of binding while a much lower $\Delta C_{p2vH} = 1.7 \pm 1.1 \text{ kJ mol}^{-1} \text{ K}^{-1}$ is found for the second step of binding. From the well-studied phenomenon of protein binding to nucleic acids we know that even nonspecific protein–ligand binding can lead to a positive heat capacity change due to proton uptake or dissociation and conformational change of the protein.^[15] For the present systems, however, a significant change of the secondary structure of an adsorbed protein can be ruled out as shown in Figure S1, Supporting Information.

Figure 5a presents also the temperature dependence of ΔG_b for the binding of HSA to dendritic polyglycerol sulfate (dPGS) studied by Ran et al.^[44] and to short PAA chains as studied by Yu et al.^[29] In all cases, a small dependence of the Gibbs free energy of binding, ΔG_b , is seen which arises from strong

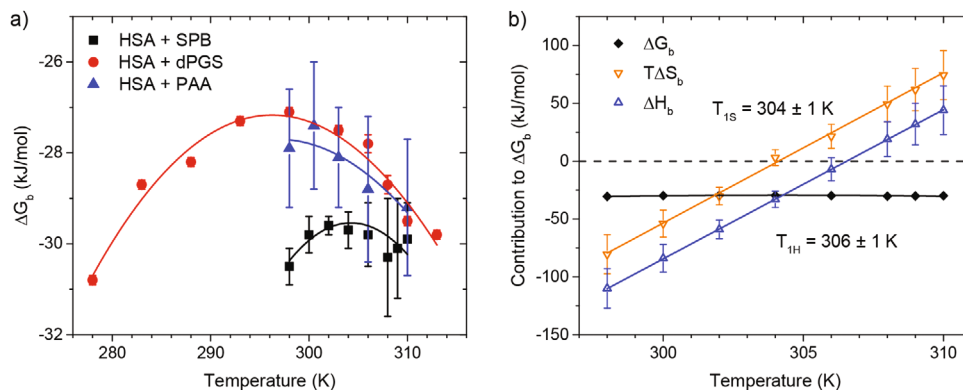


Figure 5. a) Temperature dependence of the ΔG_b for the first step of binding of HSA onto SPB (black dots). Red points and blue triangles represent the temperature dependence of the ΔG_b for the binding of HSA to charged dendrimers (dPGS)^[44] and short PAA chains,^[29] respectively. Solid lines represent the fitting obtained from the integrated form of the nonlinear van't Hoff equation (Equation (12)). b) Changes in the thermodynamic parameters (ΔG_b , ΔH_b , $T\Delta S_b$) that accompany the first step of binding of HSA onto SPB as a function of temperature. Black squares show the binding free energy. The solid black line shows the theoretical fit of ΔG_b (Equation (12)); $T\Delta S_b$ is shown as the orange line and ΔH_b is shown as the blue line.

enthalpy–entropy cancellation, as further discussed below. The same observation has been made for a large number of biochemical systems^[10,13,15,16,46] and for studies on the interaction of charged dendrimers with proteins.^[44,45] Figure 5b displays all thermodynamic parameters obtained for the first step of binding of HSA to the SPB. The characteristic temperatures found for this system are, $T_{1S} \approx 304 \text{ K}$ and $T_{1H} \approx 306 \text{ K}$.

The discrepancies between ΔH^{ITC} and ΔH_b (see Table S1, Supporting Information) are significant for both steps and the calorimetric values ΔH^{ITC} are greater than values resulting from the van't Hoff analysis. Similar findings were previously observed in the case of protein interacting with microgels,^[39] short polyelectrolytes,^[29] and charged dendrimers.^[45] It was shown that the van't Hoff enthalpy ΔH_b can significantly deviate from the calorimetric enthalpy ΔH^{ITC} and may even change sign.^[45] This discrepancy can be traced back to linked equilibria such as buffer ionization^[16] or to hydration of counterions freed upon binding.^[29] This point can be verified by comparison of buffers with different heats of ionization, as presented earlier.^[39,45]

The enthalpy and the entropy obtained is displayed in Figure 6a. The linearity of the data in Figure 6a indicates a strong enthalpy–entropy compensation. The resulting fit is given by the following equations:

$$\Delta H_{b1} = -30.4 + 1.0 \cdot T\Delta S_{b1} \quad (1)$$

and

$$\Delta H_{b2} = -18.3 + 0.9 \cdot T\Delta S_{b2} \quad (2)$$

for the first and the second step (see Figure S10, Supporting Information) of binding, respectively. The value of the intercept at zero $T\Delta S_b$ represents the average binding free energy.

The slope close to unity indicates that the entropy factor compensates the enthalpy nearly fully over a range of $\approx 170 \text{ kJ mol}^{-1}$ in the first step of binding and over a range of $\approx 20 \text{ kJ mol}^{-1}$ in the second step of binding. Figure 6a also shows the comparison with the binding of HSA to dPGS and short PAA chains, and shows that the EEC found in those systems is directly

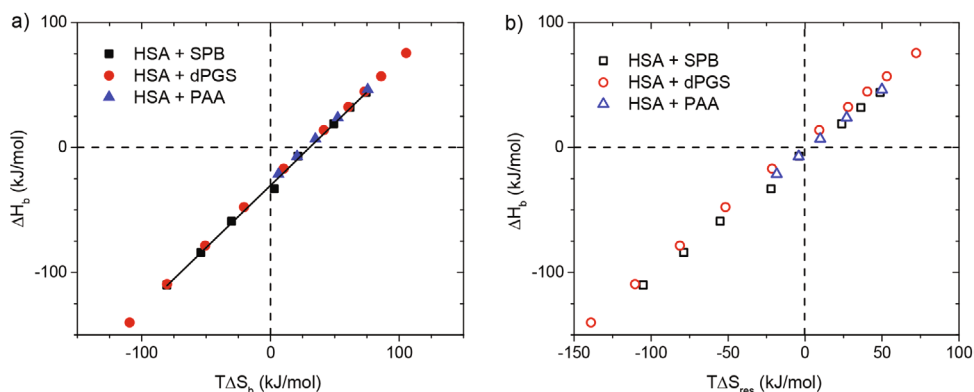


Figure 6. a) Energetics of HSA binding to SPB. Dependence of the enthalpy, ΔH_b , on the entropy factor, $T\Delta S_b$, in the first step of binding presented as black dots. The solid black line shows the linear fit resulting from Equation (1). Red points and blue triangles represent the energetics of interaction of HSA with dPGS and short PAA chains, respectively. b) Enthalpy–entropy cancellation. The binding enthalpy, ΔH_b , is plotted against $T\Delta S_{res}$ according to Equation (6).

comparable to that in the present study of HSA interacting with SPBs.

In summary, we conclude that the small dependence of the free energy of binding on temperature and the concomitant EEC is indeed a general phenomenon that occurs also in more complicated systems such as the HSA binding to SPBs, as shown here. All data evaluated so far point to the fact that the binding of a protein to a polyelectrolyte is always accompanied by EEC.

Thus, the full set of thermodynamic data can now be analyzed in an entirely quantitative manner following a suggestion by Dragan et al.^[10] The binding energy is split into

$$\Delta G_b = \Delta G_{res} + \Delta G_{ci} \quad (3)$$

where ΔG_{res} is the residual of the Gibbs free energy of binding deriving from the binding constant K_b (1 M) extrapolated to 1 M salt concentration, whereas ΔG_{ci} denotes the part related to counterion release.^[10] Since counterion release is an entirely entropic effect we get,^[5]

$$\Delta G_{ci} \approx -T\Delta S_{ci} = -\Delta N_{ci} \cdot k_b T \cdot \ln\left(\frac{c_{si}}{c_s}\right) \quad (4)$$

where ΔS_{ci} represents the change of entropy of the counterions, ΔN_{ci} denotes the number of released counterions,^[44] and c_{si} and c_s are the concentrations of condensed and bulk counterions, respectively. As discussed above, the first step of binding we observed here is related to the adsorption of one HSA molecule per PAA chain. For our analysis here we can therefore use the value of $\Delta N_{ci} = 3.0 \pm 0.5$, previously furnished by Yu et al.^[29] The concentration of condensed counterions on a linear PAA-chain may be estimated at ambient temperature according to Manning by,^[19]

$$c_{si} = 24.3 \cdot (\xi \cdot b^3)^{-1} \quad (5)$$

where b is the distance between two charges along the chain expressed in angstroms. For a PAA chain $b = 2.5$ Å. The quantity ξ represents the charge parameter which is the ratio of the

Bjerrum length to b .^[19] For water at 25 °C, $\xi = (7.1 \cdot b^{-1})$.^[19] For PAA chains under these conditions the $c_{si} \approx 0.55$ mol L⁻¹. Note, this concentration is independent of c_s .^[19]

If the total binding entropy $\Delta S_b(T)$ is known for different temperatures, its residual part $\Delta S_{res}(T)$ can be obtained from,^[10]

$$\Delta S_{res}(T) = \Delta S_b(T) - \Delta S_{ci}(T) \quad (6)$$

Figure 6b plots ΔH_b as a function of $T\Delta S_{res}$ obtained from Equation (6) (see Table S2, Supporting Information). The plot leads to comparable data for these systems. The intercept located near zero represents the average value of ΔG_{res} . Its small value demonstrates that the counterion release is the only decisive contribution that leads to the binding of HSA to short polyelectrolyte chains, charged dendrimers and spherical polyelectrolyte brushes.

In the present work we describe the analysis of the binding of human serum albumin (HSA) onto spherical polyelectrolyte brushes (SPBs), studied by isothermal titration calorimetry (ITC). Our experiments show that HSA adsorption onto SPBs can be described with a two-step model. Moreover, our analysis revealed that the counterion release entropy is the main contribution to the binding free energy. ITC measurements, performed over a range of temperatures between 25 and 37 °C show a strong temperature dependence of the calorimetric enthalpy (ΔH^{ITC}) along with a nearly temperature-invariant binding free energy (ΔG_b). A nonlinear van't Hoff analysis demonstrates that this system exhibits a marked enthalpy–entropy cancellation. The comparison of the present results with a large set of data from other systems^[5,10,12,14,29,44,45] show that a strong enthalpy–entropy cancellation is a general feature occurring in systems in which the binding is dominated by counterion release.

Following Dragan et al.^[10] the data gathered so far strongly suggest that the EEC is an entirely non-electrostatic phenomenon that is related to the uptake and the release of water molecules during binding. Thus, uptake of water leads to a gain in enthalpy of binding but also to a concomitant loss of entropy. For water at room temperature, enthalpy and entropy cancel each other out to very good approximation.

Experimental Section

Materials: Styrene and acrylic acid (AAc) monomers, the potassium persulfate (KPS) initiator, and the sodium dodecyl sulfate (SDS) emulsifier were all purchased from Sigma-Aldrich. Styrene was flushed over a column filled with inhibitor remover (Sigma-Aldrich). AAc was distilled under reduced pressure (1 mbar, 40–45 °C) in a rotary evaporator to remove the stabilizer hydroquinone monomethylether. KPS and SDS as well as photoinitiator 2-[*p*-(2-hydroxy-2-methylpropiophenone)]-ethylene glycol-methacrylate (HMEM) for the synthesis of core-shell particles were used as received. Albumin from human serum and all components used for buffer preparation, that is, 3-(*N*-morpholino) propane sulfonic acid (MOPS) and sodium chloride (NaCl), were received from Sigma-Aldrich and used without further purification.

Synthesis and Characterization of the SPB: The SPB-PAA were synthesized by conventional photoemulsion polymerization following a well-established procedure.^[47] The radius of the core-brush particles is 286 ± 20 nm as determined by dynamic light scattering (DLS at 298 K in 10 mM MOPS buffer, pH 7.2 and $l = 20$ mm adjusted by NaCl). The molecular weight M_w of the particles was calculated to be 5.56×10^8 g mol⁻¹ with Equation (7), using data obtained from ultrafiltration measurements.

$$M_w = (m_{\text{core}} + m_{\text{brush}})N_A = \frac{\left(\rho_{\text{core}} \frac{4}{3}\pi(R_{h,\text{core}})^3\right)}{w_{\text{core}}} N_A \quad (7)$$

where ρ_{core} is the density of the PS core (1.055 g cm⁻³)^[39] and $R_{h,\text{core}}$ is the hydrodynamic radius of the PS core determined by DLS. The mass of acrylic acid not built into the brush was determined from the mass balance of the SPB dispersion before and after purification and the mass fraction of the core was calculated via Equation (8) and accounted for 65% of the added monomer.

$$w_{\text{core}} = \frac{m_{\text{core}}}{m_{\text{brush}} + m_{\text{core}}} \quad (8)$$

To determine the grafting density σ of the attached chains, samples of the SPB latex were hydrolyzed to cleave the PAA chains from the surface of the PS particles.^[47] After heating at 97 °C in 2 M aqueous NaOH for 17 days, the latex coagulated due to the loss of the steric stabilization by the PAA chains. The PAA chains thus obtained were separated by centrifugation. Measurements of the intrinsic viscosity $[\eta]$ in 2 M NaOH at 25 °C using an Ubbelohde viscometer gave the viscosity average molecular weight $[M\eta]$ of the PAA chains. Here, the Mark-Houwink relation for PAA in aqueous 2 M NaOH ($K = 4.22 \times 10^{-2}$ mL g⁻¹, $\alpha = 0.64$) has been used.^[48,49] $M\eta = 96000$ g mol⁻¹ and $\sigma = 0.013$ nm⁻². Hence, the average number of PAA-chains per SPB particle is ≈ 540 .

Isothermal Titration Calorimetry: ITC experiments were conducted using a Microcal VP-ITC instrument (Microcal, Northampton, MA). All samples used in the measurements were prepared in a buffer solution of 10 mM MOPS and 10 mM NaCl to adjust the ionic strength. The pH of each solution was fixed to 7.2. A total of 280 μ L of HSA-buffer solution was titrated into the cell containing 1.4 mL of SPB solution in 94 successive 3 μ L injections while stirring at 307 rpm and a time interval of 360 s between each injection. The concentrations of HSA were as follows: 24.0, 35.0, and 45.0 g L⁻¹, and the concentrations of SPB were varied from 1.38 to 1.84 g L⁻¹. These concentrations were chosen to obtain more data points at lower molar ratios while increasing temperature. The measurements were performed at 25, 27, 29, 31, 33, 35, 36 and 37 °C and at an ionic strength of 20 mM. All samples were degassed and thermostated for several minutes at 1° below the experimental temperature before the ITC-measurements. Details on the data analysis can be found in the supporting information.

In the following, the evaluation of ITC data is demonstrated for the adsorption of HSA onto SPBs at $T = 27$ °C. Special emphasis was given to the subtraction of the heat of dilution. **Figure 7a** shows the raw-ITC signal of adsorption (black curves and circles) and dilution of HSA (green curves and points). The heat of dilution of HSA was subtracted from the heat of adsorption. For some cases, the subtraction of the heat of dilution of HSA was insufficient because at lower protein

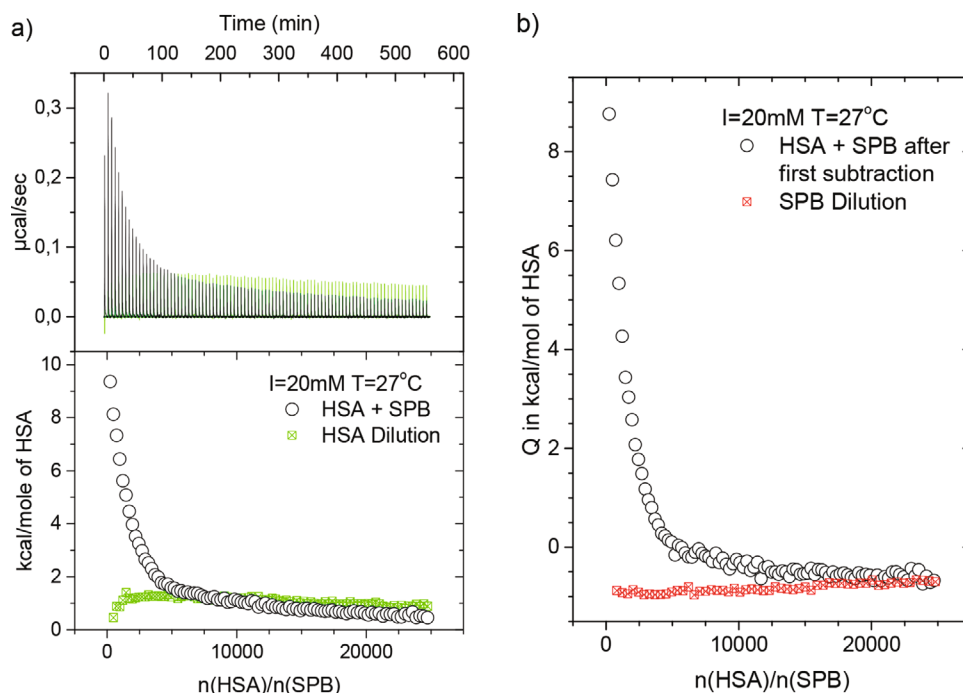


Figure 7. a) ITC data for the adsorption of HSA onto SPBs at pH 7.2, $l = 20$ mm, $T = 27$ °C. The upper panel shows the raw data of the adsorption of HSA onto SPBs (black curves) and the dilution of HSA by buffer (green curves). The integrated heats of each injection are shown in the lower panel. b) Integrated heats of each injection after first subtraction (corrected for protein heat of dilution) (black circles) and the dilution of SPBs by buffer (red points).

concentration (24 g L⁻¹) a considerable heat effect caused by the heat of dilution of SPB itself was observed. Therefore a double subtraction for measurements was performed at low protein concentration. Hence, after subtracting the heat of dilution of HSA from the heat of adsorption (see Figure 7b, black circles) the heat of dilution of SPB was subtracted (see Figure 7b, red points). In this way, ITC-measurements can be performed also under conditions in which the signal from the binding process has become rather weak.

Enthalpy–Entropy Cancellation: The compensation of enthalpy by entropy (EEC) is a well-known and ubiquitous phenomenon that occurs in virtually all systems where a highly charged polyelectrolyte interacts with a protein. The EEC^[14,30,50–53] has been the subject of a long debate.^[32,54,55] Li et al. presented a thorough analysis of a large number of experimental data and showed that EEC is based on solid experimental evidence.^[56] Careful experimental studies conducted by the Whitesides group explained EEC by the reformation of the water network around the complex.^[55] Moreover, Jen-Jacobson and coworkers performed a series of carefully conducted experiments on systems of biological relevance.^[14,52,57,58] These investigations also showed that EEC exists in these systems. In the following the exposition of EEC by Jen-Jacobson and coworkers is followed.^[52]

For a system characterized by a specific heat capacity change, ΔC_p , that is much larger than the binding entropy, ΔS_b , $|\Delta C_p| \gg |\Delta S_b|$ we get the relations,^[52]

$$\Delta H_b \approx \Delta C_p \cdot (T - T_H) \quad (9)$$

$$T\Delta S_b \approx \Delta C_p \cdot (T - T_S) \quad (10)$$

and

$$\Delta G_b \approx \Delta C_p \cdot (T_S - T_H) \quad (11)$$

Here, ΔH_b and ΔS_b denote the enthalpy and the entropy of binding, respectively, and T_H and T_S are the temperatures where $\Delta H_b = 0$ or $\Delta S_b = 0$, respectively. These relations clearly show that ΔG_b is approximately a constant in a range of temperatures where both ΔH_b and ΔS_b are small and change their sign. Therefore the EEC will always occur when T_H and T_S are located near the experimental temperature. With these prerequisites, the dependence of ΔG_b on temperature T is given by the nonlinear van't Hoff equation,^[13,16,59,60]

$$\Delta G_b = \Delta H_{b,ref} - T\Delta S_{b,ref} + \Delta C_p \left(T - T_{ref} - T \cdot \ln \left(\frac{T}{T_{ref}} \right) \right) \quad (12)$$

where the Gibbs free energy of binding, ΔG_b , is given by

$$\Delta G_b = -RT \ln K_b \quad (13)$$

Here, T_{ref} denotes a reference temperature that can be chosen freely. Fits of Equation (12) to experimental data of ΔG_b as a function of T then lead to the molar heat capacity change, ΔC_p , and to ΔH_b and ΔS_b .

Supporting Information

Supporting Information is available from the Wiley Online Library or from the author.

Acknowledgements

The authors are grateful for financial support from the Deutsche Forschungsgemeinschaft via the International Research Training Group 1524 and for financial support from National Science Foundation Research Triangle Materials Research Science and Engineering Center

(NSF MRSEC, DMR-11211107). The authors acknowledge helpful discussions with J. Dzubiella.

Conflict of Interest

The authors declare no conflict of interest.

Keywords

Spherical polyelectrolyte brushes, proteins, ITC, thermodynamics, enthalpy–entropy compensation (EEC)

Received: August 15, 2019

Revised: September 19, 2019

Published online: November 7, 2019

- [1] C. G. De Kruijff, F. Weinbreck, R. De Vries, *Curr. Opin. Colloid Interface Sci.* **2004**, *9*, 340.
- [2] A. Wittemann, M. Ballauff, *Phys. Chem. Chem. Phys.* **2006**, *8*, 5269.
- [3] A. L. Becker, K. Henzler, N. Welsch, M. Ballauff, O. Borisov, *Curr. Opin. Colloid Interface Sci.* **2012**, *17*, 90.
- [4] a. B. Kayitmazer, D. Seeman, B. B. Minsky, P. L. Dubin, Y. Xu, *Soft Matter* **2013**, *9*, 2553.
- [5] X. Xu, S. Angioletti-Uberti, Y. Lu, J. Dzubiella, M. Ballauff, *Langmuir* **2019**, *35*, 5373.
- [6] X. Du, P. L. Dubin, D. a. Hoagland, L. Sun, *Biomacromolecules* **2014**, *15*, 726.
- [7] E. Kizilay, A. B. Kayitmazer, P. L. Dubin, *Adv. Colloid Interface Sci.* **2011**, *167*, 24.
- [8] M. T. Record, C. F. Anderson, T. M. Lohman, *Q. Rev. Biophys.* **1978**, *11*, 103.
- [9] T. M. Lohman, W. Bujalowski, *Biochemistry* **1994**, *33*, 6167.
- [10] A. I. Dragan, C. M. Read, C. Crane-Robinson, *Eur. Biophys. J.* **2017**, *46*, 301.
- [11] T. Sasaki, Y. Kanke, M. Nagahashi, M. Toyokawa, M. Matsuda, J. Shimizu, Y. Misawa, T. Takita, *J. Agric. Food Chem.* **2000**, *48*, 1047.
- [12] K. Datta, A. J. Wowor, A. J. Richard, V. J. LiCata, *Biophys. J.* **2006**, *90*, 1739.
- [13] K. Datta, V. J. LiCata, *Nucleic Acids Res.* **2003**, *31*, 5590.
- [14] L. Jen-Jacobson, L. E. Engler, J. T. Ames, M. R. Kurpiewski, A. Grigorescu, *Supramol. Chem.* **2000**, *12*, 143.
- [15] A. Niedzwiecka, J. Stepinski, E. Darzynkiewicz, N. Sonenberg, R. Stolarski, *Biochemistry* **2002**, *41*, 12140.
- [16] A. Niedzwiecka, E. Darzynkiewicz, R. Stolarski, *Biochemistry* **2004**, *43*, 13305.
- [17] P. L. Privalov, *J. Solution Chem.* **2015**, *44*, 1141.
- [18] J. Janin, A. M. Bonvin, *Curr. Opin. Struct. Biol.* **2013**, *23*, 859.
- [19] G. S. Manning, *Q. Rev. Biophys.* **1978**, *11*, 179.
- [20] Y. B. Yu, P. Lavigne, C. M. Kay, R. S. Hodges, P. L. Privalov, *J. Phys. Chem. B* **1999**, *103*, 2270.
- [21] P. L. Privalov, A. I. Dragan, C. Crane-Robinson, *Nucleic Acids Res.* **2011**, *39*, 2483.
- [22] X. Xu, Q. Ran, P. Dey, R. Nikam, R. Haag, M. Ballauff, J. Dzubiella, *Biomacromolecules* **2018**, *19*, 409.
- [23] A. Wittemann, B. Haupt, M. Ballauff, *Phys. Chem. Chem. Phys.* **2003**, *5*, 1671.
- [24] A. Wittemann, B. Haupt, M. Ballauff, *Prog. Colloid Polym. Sci.* **2006**, *133*, 58.
- [25] K. Henzler, B. Haupt, K. Lauterbach, A. Wittemann, O. Borisov, M. Ballauff, *J. Am. Chem. Soc.* **2010**, *132*, 3159.



- [26] K. Henzler, A. Wittemann, E. Breininger, M. Ballauff, S. Rosenfeldt, *Biomacromolecules* **2007**, *8*, 3674.
- [27] K. Henzler, B. Haupt, S. Rosenfeldt, L. Harnau, T. Narayanane, M. Ballauff, *Phys. Chem. Chem. Phys.* **2011**, *13*, 17599.
- [28] C. Yigit, M. Kanduć, M. Ballauff, J. Dzubiella, *Langmuir* **2017**, *33*, 417.
- [29] S. Yu, X. Xu, C. Yigit, M. van der Giet, W. Zidek, J. Jankowski, J. Dzubiella, M. Ballauff, *Soft Matter* **2015**, *11*, 4630.
- [30] R. Lumry, S. Rajender, *Biopolymers* **1970**, *9*, 1125.
- [31] S. Vega, O. Abian, A. Velazquez-Campoy, *Biochim. Biophys. Acta, Gen. Subj.* **2016**, *1860*, 868.
- [32] S. Geschwindner, J. Ulander, P. Johansson, *J. Med. Chem.* **2015**, *58*, 6321.
- [33] M. Ballauff, *Prog. Polym. Sci.* **2007**, *32*, 1135.
- [34] Y. Lu, M. Ballauff, A. Wittemann, *Polym. Sci. A Compr. Ref. 10 Vol. Set* **2012**, *6*, 265.
- [35] N. Welsch, Y. Lu, J. Dzubiella, M. Ballauff, *Polymer* **2013**, *54*, 2835.
- [36] A. Wittemann, M. Ballauff, *Anal. Chem.* **2004**, *76*, 2813.
- [37] A. Wittemann, M. Ballauff, *Macromol. Biosci.* **2005**, *5*, 13.
- [38] S. Yu, M. Schuchardt, M. Tölle, M. van der Giet, W. Zidek, J. Dzubiella, M. Ballauff, *RSC Adv.* **2017**, *7*, 27913.
- [39] N. Welsch, A. L. Becker, J. Dzubiella, M. Ballauff, *Soft Matter* **2012**, *8*, 1428.
- [40] G. Jackler, A. Wittemann, M. Ballauff, C. Czeslik, *Spectroscopy* **2004**, *18*, 289.
- [41] N. Welsch, A. Wittemann, M. Ballauff, *J. Phys. Chem. B* **2009**, *113*, 16039.
- [42] A. Wittemann, B. Haupt, M. Ballauff, *Phys. Chem. Chem. Phys.* **2003**, *5*, 1671.
- [43] C. L. Cooper, A. Goulding, A. Basak Kayitmazer, S. Stoll, S. Turksen, S. I. Yusa, A. Kumar, P. L. Dubin, *Biomacromolecules* **2006**, *7*, 1025.
- [44] Q. Ran, X. Xu, P. Dey, S. Yu, Y. Lu, J. Dzubiella, R. Haag, M. Ballauff, *J. Chem. Phys.* **2018**, *149*, 163324.
- [45] Q. Ran, X. Xu, J. Dzubiella, R. Haag, M. Ballauff, *ACS Omega* **2018**, *3*, 9086.
- [46] K. Datta, V. J. LiCata, *J. Biol. Chem.* **2003**, *278*, 5694.
- [47] X. Guo, A. Weiss, M. Ballauff, *Macromolecules* **1999**, *32*, 6043.
- [48] X. Guo, M. Ballauff, *Langmuir* **2000**, *16*, 8719.
- [49] X. Wang, S. Wu, L. Li, R. Zhang, Y. Zhu, M. Ballauff, Y. Lu, X. Guo, *Ind. Eng. Chem. Res.* **2011**, *50*, 3564.
- [50] J. H. Ha, R. S. Spolar, M. T. Record, *J. Mol. Biol.* **1989**, *209*, 801.
- [51] R. S. Spolar, J. H. Ha, M. T. Record, *Proc. Natl. Acad. Sci. USA* **1989**, *86*, 8382.
- [52] L. Jen-Jacobson, L. E. Engler, L. A. Jacobson, *Structure* **2000**, *8*, 1015.
- [53] G. Klebe, *Nat. Rev. Drug Discovery* **2015**, *14*, 95.
- [54] J. D. Chodera, D. L. Mobley, *Annu. Rev. Biophys.* **2013**, *42*, 121.
- [55] J. M. Fox, M. Zhao, M. J. Fink, K. Kang, G. M. Whitesides, *Annu. Rev. Biophys.* **2018**, *47*, 223.
- [56] L. Li, J. J. Dantzer, J. Nowacki, B. J. O'Callaghan, S. O. Meroueh, *Chem. Biol. Drug Des.* **2008**, *71*, 529.
- [57] L. E. Engler, P. Sapienza, L. F. Dorner, R. Kucera, I. Schildkraut, L. Jen-Jacobson, *J. Mol. Biol.* **2001**, *307*, 619.
- [58] P. J. Sapienza, T. Niu, M. R. Kurpiewski, A. Grigorescu, L. Jen-Jacobson, *J. Mol. Biol.* **2014**, *426*, 84.
- [59] Y. Liu, J. M. Sturtevant, *Biophys. Chem.* **1997**, *64*, 121.
- [60] D. J. Winzor, C. M. Jackson, *J. Mol. Recognit.* **2006**, *19*, 389.